

Gaussian Process Tilted Nonparametric Density Estimation using Fisher Divergence Score Matching

John Paisley
Columbia University
New York, NY, USA

Wei Zhang
Columbia University
New York, NY, USA

Brian Barr
Capital One Labs
New York, NY, USA

Abstract—We present three Fisher divergence (FD) minimization algorithms for learning Gaussian process (GP) based score models for lower dimensional density estimation problems. The density is formed by multiplying a base multivariate normal distribution with an exponentiated GP refinement, and so we refer to it as a GP-tilted nonparametric density. By representing the GP part of the score as a linear function using the random Fourier feature (RFF) approximation, we show that all learning problems can be solved in closed form. This includes the basic and noise conditional versions of the Fisher divergence, as well as a novel alternative to noise conditional FD models based on variational inference (VI). Here, we propose using an ELBO-like optimization of the approximate posterior with which we derive a *Fisher variational predictive distribution*. The RFF representation of the GP, which is functionally equivalent to a single layer neural network score model with cosine activation, provides a unique linear form for which all expectations are in closed form. The Gaussian base also helps with tractability of the VI approximation. We demonstrate our three learning algorithms, as well as a MAP baseline algorithm, on several low dimensional density estimation problems. The closed-form nature of the learning problem removes the reliance on iterative algorithms, making this technique particularly well-suited to large data sets.

I. INTRODUCTION

Density estimation is a fundamental component of generative modeling. With deep neural networks, density estimation has been significantly improved using autoregressive models [1, 2, 3, 4], VAEs [5, 6], energy-based models [7], normalizing flows [8, 9, 10, 11] and GANs [12].

Parallel to these developments, score-based methods have emerged as a powerful learning approach for generative models [13]. Instead of optimizing the log-likelihood of the data, it uses the Fisher divergence between the model and data distributions to match the log gradients of the two distributions,

$$\mathbb{E}_{x \sim p_{\text{data}}(x)} [\|\nabla_x \log p(x) - s_\theta(x)\|^2]. \quad (1)$$

The gradient of the log density, $s_\theta(x)$, which is called the (Stein) score function [14], approximates those of the true data distribution. Often this function is a complex neural network with parameters θ . Many works have been proposed to optimize this divergence [15, 16, 17]. New data samples are generated from $p_\theta(x) \propto \exp\{\int s_\theta(x)dx\}$ with Langevin dynamics. To avoid an indefinite integral we use $\nabla_x s_\theta(x)$ in (1).

The advantages of using Fisher divergence for score matching have been demonstrated for breaking the curse of dimensionality [18] and solving general inverse problems [19], such

as compressed sensing MRI [20]. An additional benefit of using score matching is that the score function $s_\theta(x)$ does not need to correspond to a textbook density and so can be any neural network function, in effect making the approximation nonparametric.

While clearly very powerful, these approaches also suffer from common limitations of learning complex networks of many parameters. In this paper, we focus on lower density estimation problems for which a simpler network is sufficient. In particular, we base our score function on a Gaussian process tilted density. Gaussian processes and tilted distributions have been shown to work well for nonparametric density estimation problems [21, 22, 23]. Kernel-based exponential family ideas have also been introduced for score matching, leading to iterative learning algorithms and deep representations [24, 25, 26, 27]. In contrast with these methods, our algorithms will have closed form solutions.

We propose a GP-tilted density estimator using the random Fourier feature approximation and learned it via Fisher divergence. Our selected GP is mathematically equivalent to a single layer fully connected neural network with randomized parameters; the only parameter to be learned is a linear layer vector with dimension equal to the approximation level of the GP. We derive a noise-conditional method and a novel variational predictive distribution for learning, both of which have closed form solutions as a result of our chosen score function. We evaluate our Fisher divergence-based algorithms, as well as MAP and kernel density estimation, on several low dimensional problems.

Our main contributions are two-fold:

- 1) Our model is equivalent to an exponentiated single layer neural network for which one parameter vector needs to be learned (on the order of 1000s of parameters). We present three different algorithms for this based on modifications of the Fisher divergence, all of which give closed form solutions for this vector, making the technique particularly well-suited for large data sets.
- 2) We propose a new approach to the Fisher divergence based on a variational approximation to the model posterior using an ELBO-like function and variational tempering. The corresponding predictive distribution on the data integrates out uncertainty in the model parameter rather than by adding noise to the data, giving

an alternative to noise-conditional Fisher divergence methods for our model.

The paper is organized as follows: In Section 2, we provide a brief background on the Gaussian process and the Fisher divergence score matching methods that is relevant for our derivations. In Section 3, we present the GP-tilted density model and derive three different, closed-form solutions for learning its parameter vector. We then demonstrate the model on several low dimensional data sets in Section 4.

II. BACKGROUND

We first briefly review background on Gaussian processes and Fisher divergence minimization that we use for our GP-tilted density estimation model and algorithms.

A. Gaussian Processes

Definition II.1 (Gaussian Process). Let $k(x, x')$ be a kernel function between two vectors $x, x' \in \mathbb{R}^D$. Then the function $f : \mathbb{R}^D \rightarrow \mathbb{R}$ is a zero-mean Gaussian process if, for any N vectors x_1, \dots, x_N , the corresponding function evaluations $[f(x_1), \dots, f(x_N)]^\top \sim \mathcal{N}(0, K_N)$, where $K_N(i, j) = k(x_i, x_j)$. We write $f(x) \sim \mathcal{GP}(0, k(x, x'))$.

There are a large variety of kernel functions k that can be used with the GP, and extensions can be made to other spaces and non-zero mean functions. The most popular kernel in general is the Gaussian kernel of the form $k(x, x') = \lambda \exp(-\frac{1}{2\gamma^2} \|x - x'\|^2)$, which measures correlations based on proximity in the input space. For the Gaussian kernel, the following random Fourier feature (RFF) definition provides an asymptotically exact way of representing the underlying linear model of the GP in its reproducing kernel Hilbert space [28]. The equivalent structure of this representation to a single layer of a neural network has recently motivated other applications of this idea to traditional machine learning problems [29, 30].

Definition II.2 (Random Fourier Features). Let S to be a positive integer, $\gamma > 0$, and $x \in \mathbb{R}^D$. For $s = 1, \dots, S$, generate $z_s \sim \mathcal{N}(0, I)$ and $c_s \sim \text{Unif}(0, 2\pi)$. The random Fourier feature mapping of the vector x is defined to be

$$\phi(x) = \sqrt{\frac{2}{S}} \left[\cos\left(\frac{z_1^\top x}{\gamma} + c_1\right), \dots, \cos\left(\frac{z_S^\top x}{\gamma} + c_S\right) \right]^\top$$

For any $x, x' \in \mathbb{R}^D$, $\phi(x)^\top \phi(x') \rightarrow \exp(-\frac{1}{2\gamma^2} \|x - x'\|^2)$ as $S \rightarrow \infty$. Thus ϕ approximates the RKHS of the GP.

It follows that the marginal of $f_\theta(x) = \theta^\top \phi(x)$ over θ , for $\theta \sim \mathcal{N}(0, \lambda^{-1}I)$, has distribution $\mathcal{GP}(0, k(x, x'))$ with $k(x, x') = \lambda^{-1} \phi(x)^\top \phi(x') \rightarrow \lambda^{-1} \exp(-\frac{1}{2\gamma^2} \|x - x'\|^2)$ in the limit as $S \rightarrow \infty$.

B. Fisher divergence for learning

Let \mathcal{P} be the true unknown distribution of data from which we have i.i.d. samples, $x \sim \mathcal{P}$. Our goal is to approximate the density $p(x)$ corresponding to \mathcal{P} with a parametric density $q_\theta(x)$. This is achieved by tuning parameters θ such that the two densities agree according to some measure of similarity.

Maximum likelihood is one standard approach based on the KL-divergence,

$$\theta_{\text{ML}} = \arg \min_{\theta} \mathbb{E}_p \left[\ln \frac{p(x)}{q_\theta(x)} \right] \approx \arg \max_{\theta} \sum_i \ln q_\theta(x_i).$$

Here, the data provides a Monte Carlo approximation.

A second method that has recently been effective for learning deep generative models is the Fisher divergence, which optimizes θ as follows,

$$\theta_{\text{FD}} = \arg \min_{\theta} \frac{1}{2} \mathbb{E}_p \|\nabla_x \ln p(x) - \nabla_x \ln q_\theta(x)\|^2. \quad (2)$$

Where a score function, typically a neural network and written in this paper as $\nabla_x \ln q_\theta(x)$, is designed to match the expected gradients of the log data distribution. Through a derivation involving integration by parts, this is equivalent to an optimization problem of the form

$$\theta_{\text{FD}} \approx \arg \min_{\theta} \frac{1}{2} \sum_{i=1}^N \|\nabla_x \ln q_\theta(x_i)\|^2 + \sum_{i=1}^N \text{trace}(\nabla_{xx}^2 \ln q_\theta(x_i)). \quad (3)$$

A Monte Carlo approximated is again made using samples $x \sim \mathcal{P}$. The Fisher score focuses on creating agreement between the derivatives of q_θ and the true distribution p in high density regions. Equation 3 shows that this is equivalent to placing a sharp mode around each x_i in q_θ .

For the GP-tilted density estimator discussed in Section III, this divergence has the advantage of producing a closed form solution for θ , in contrast to maximum likelihood (see Section III-A). As with deep generative models, the same practical issue of accurately learning the low density regions arises, which we address in two ways: In Section III-B we adopt the frequently used noise conditional representation that still has a closed-form solution, and in Section III-C we propose a variational approximation to the predictive distribution that also has a closed-form solution.

III. GP-TILTED DENSITY ESTIMATION

Let $f(x) \sim \mathcal{GP}(0, k(x, x'))$, where k is a Gaussian kernel. We define the GP-tilted (TGP) density of $x \in \mathbb{R}^D$ to be

$$q(x) = \frac{\exp\{f(x)\} \mathcal{N}(x|\mu, \Sigma)}{\int \exp\{f(x)\} \mathcal{N}(x|\mu, \Sigma) dx}. \quad (4)$$

As follows from Gaussian process theory and basic analysis, $q(x)$ is a continuous density [31]. The multivariate Gaussian base measure is used to ensure integrability of the numerator in \mathbb{R}^D . The mean μ and covariance Σ broadly define the region of the data, while the exponentiated GP provides a nonparametric refinement. Using the RFF representation of $f(x)$ in Definition II.2, this density can be approximated by

$$\begin{aligned} q_\theta(x) &\propto \exp\{\theta^\top \phi(x)\} \mathcal{N}(x|\mu, \Sigma), \\ \theta &\sim \mathcal{N}(0, \lambda^{-1}I), \end{aligned} \quad (5)$$

where ϕ is the S -dimensional random mapping. MAP inference for this model is straightforward, which we present in Algorithm 1 for reference. Functionally, the score $\ln q_\theta(x)$ has the form of a single layer neural network using RFF parameters. We next show that this approximation also allows for easy inference using Fisher divergence minimization.

Algorithm 1 MAP inference for GP tilted density estimation

Require: Data $x \in \mathbb{R}^D$, $\gamma > 0$, $\lambda > 0$, $S_1, S_2 \in \mathbb{Z}_+$, base parameters $\mu \in \mathbb{R}^D$, $\Sigma \in \mathbb{S}_{++}^d$, step size ρ

- 1: Sample $z_s \sim \mathcal{N}(0, I_d)$, $c_s \sim \text{Unif}(0, 2\pi)$, $s = 1 : S_1$
- 2: Set $\psi_1 = \sum_i \phi(x_i)$, sample $\zeta_j \sim \mathcal{N}(\mu, \Sigma)$, $j = 1 : S_2$
- 3: **for** iteration $t = 1, \dots, T$ **do**
- 4: Set $\theta_{t+1} = (1 - \rho\lambda)\theta_t + \rho(\psi_1 - N\psi_2)$,
 $\psi_2 = \sum_j \phi(\zeta_j)w_t(j)$,
- 5: $w_t(j) = \exp\{\theta_t^\top \phi(\zeta_j)\} / \sum_{j'} \exp\{\theta_t^\top \phi(\zeta_{j'})\}$
- 6: **end for**
- 7: **return** θ , Z , c , γ , μ , Σ

A. Fisher Divergence Score Matching

We recall that minimizing the Fisher divergence between the GP-tilted density and the true data density using i.i.d. samples entails working with the function

$$\mathcal{L} = \frac{1}{2} \sum_i \|\nabla_x \ln q_\theta(x_i)\|^2 + \sum_i \text{tr}(\nabla_{xx}^2 \ln q_\theta(x_i)). \quad (6)$$

(We account for the prior on θ later.) The gradient and Hessian of $\ln q_\theta(x)$ in our case are

$$\nabla_x \ln q_\theta(x) = \sum_s \frac{1}{\gamma} \theta_s \phi'_s(x) z_s - \Sigma^{-1}(x - \mu), \quad (7)$$

$$\nabla_{xx}^2 \ln q_\theta(x) = \sum_s \frac{1}{\gamma^2} \theta_s \phi''_s(x) z_s z_s^\top - \Sigma^{-1}, \quad (8)$$

where for $s = 1, \dots, S$ we have defined

$$\begin{aligned} \phi'_s(x) &= -\sqrt{2/S} \sin(z_s^\top x / \gamma + c_s), \\ \phi''_s(x) &= -\sqrt{2/S} \cos(z_s^\top x / \gamma + c_s). \end{aligned} \quad (9)$$

As is evident, after plugging Eqs. 7 & 8 into Equation 6, the Fisher divergence is a quadratic-plus-linear function of θ . Define the matrix $Z = [z_1, \dots, z_S]^\top$ and for any square matrix M , let $\|ZM\|^2 \equiv (\|Mz_1\|^2, \dots, \|Mz_S\|^2)^\top$ — in this subsection, $M = I$. Optimizing for θ requires the following gradient,

$$\begin{aligned} \nabla_\theta \mathcal{L} &= \left(\sum_{i=1}^N \frac{1}{\gamma^2} Z Z^\top \odot \phi'(x_i) \phi'(x_i)^\top \right) \theta \\ &\quad - \sum_{i=1}^N \frac{1}{\gamma} \phi'(x_i) \odot Z \Sigma^{-1} (x_i - \mu) \\ &\quad + \sum_{i=1}^N \frac{1}{\gamma^2} \phi''(x_i) \odot \|Z\|^2, \end{aligned} \quad (10)$$

where \odot indicates elementwise multiplication.

We also recall that the Gaussian prior of the linearized GP is $\theta \sim \mathcal{N}(0, \lambda^{-1}I)$. This introduces an ℓ_2 regularization term, $\theta_{\text{FD}} = \arg \min_\theta \mathcal{L}(\theta) + \frac{\lambda}{2} \theta^\top \theta$. Finally, using the fact that $\phi'' = -\phi$, the value of θ that minimizes this function is

$$\theta_{\text{FD}} = (\lambda \gamma^2 I + Z Z^\top \odot \sum_i \phi'(x_i) \phi'(x_i)^\top)^{-1} \times \left(\sum_i \gamma \phi'(x_i) \odot Z \Sigma^{-1} (x_i - \mu) + \phi(x_i) \odot \|Z\|^2 \right). \quad (11)$$

This involves inverting an $S \times S$ matrix, where S is the number of random Fourier features used to approximate the Gaussian process. When large values of S or other numerical issues present a computational challenge, conjugate gradients can be used to quickly solve for θ instead. We summarize parameter estimation for the basic GP-tilted density using Fisher divergence in Algorithm 2.

Algorithm 2 Fisher divergence for TGP learning

Require: Data $x \in \mathbb{R}^D$, kernel width $\gamma > 0$, param $\lambda > 0$, $S \in \mathbb{Z}_+$, base parameters $\mu \in \mathbb{R}^D$, $\Sigma \in \mathbb{S}_{++}^d$

- 1: Sample $z_s \sim \mathcal{N}(0, I_d)$, $c_s \sim \text{Unif}(0, 2\pi)$, $s = 1 : S$
- 2: Def $Z = [z_1, \dots, z_S]^\top$, $\|Z\|^2 = (\|z_1\|^2, \dots, \|z_S\|^2)^\top$
- 3: Construct each $\phi'(x_i)$ and $\phi(x_i) = -\phi''(x_i)$ (Eq. 9)
- 4: Using all data, calculate

$$\begin{aligned} \Phi' &= \sum_i \phi'(x_i) \phi'(x_i)^\top \\ \psi' &= \sum_i \phi'(x_i) \odot Z \Sigma^{-1} (x_i - \mu) \\ \psi &= \sum_i \phi(x_i) \end{aligned}$$

5: Solve either directly or, e.g., with conjugate gradients,

$$\theta_{\text{FD}} = (\lambda \gamma^2 I + Z Z^\top \odot \Phi')^{-1} (\gamma \psi' + \|Z\|^2 \odot \psi).$$

return θ_{FD} , Z , c , γ , μ , Σ

1) *Learning base measure parameters μ and Σ :* The base Gaussian measure of $q_\theta(x)$ in Equation 5 is important because it defines the region of focus for the Gaussian process. When set too small, the base resists the GP's ability to increase the density near data outside this region. When it is too large, it requires the GP to be learned well in regions of no data, which isn't likely since the GP $\theta^\top \phi(x)$ reverts to something like evaluations of the random prior. This can randomly produce large positive values away from the data that dominate the overall density $q_\theta(x)$.

We propose two modifications to address this issue in Section III-B and Section III-C. Here we note that, when optimizing the basic objective function in Equation 6, we can also include optimization over μ and Σ as follows: For $\mu = \arg \min_\mu \mathcal{L}$, the optimal value given θ and Σ is

$$\mu = \frac{1}{N} \left[\sum_{i=1}^N x_i \right] - \frac{1}{\gamma} \Sigma Z^\top (\theta \odot \frac{1}{N} \sum_{i=1}^N \phi'(x_i)). \quad (12)$$

Differentiating to find $\Sigma = \arg \min_\Sigma \mathcal{L}$, we obtain the Lyapunov equation $\bar{\Sigma} \Sigma^{-1} + \Sigma^{-1} \bar{\Sigma} = Q$, where

$$\bar{\Sigma} = \frac{1}{N} \sum_{i=1}^N (x_i - \mu)(x_i - \mu)^\top, \quad (13)$$

$$\Upsilon = \frac{1}{N} \sum_{i=1}^N (\theta \odot \phi'(x_i))(x_i - \mu)^\top, \quad (14)$$

$$Q = 2I + (Z^\top \Upsilon + \Upsilon^\top Z) / \gamma. \quad (15)$$

This also has a closed form solution using the Kronecker product as follows,

$$\text{vec}(\Sigma^{-1}) = (\bar{\Sigma} \otimes I + I \otimes \bar{\Sigma})^{-1} \text{vec}(Q). \quad (16)$$

For data $x \in \mathbb{R}^D$, this matrix inverse is $\mathcal{O}(D^6)$. This is not prohibitive for the low dimensional problems we focus on. As the dimensionality increases, other algorithms can be used to solve for Σ . When optimizing Equation 6, the base parameters can be learned by iterating between updates to θ (Algorithm 2) and μ and Σ (Equations 12 & 16), with slower runtime because the algorithm is now iterative.

B. Noise Conditional Score Matching

It has often been observed that the approach of Section III-A will have difficulty accurately learning q_θ in regions where

little or no data exists, which can lead to inflated density values in low data regions as a learning artifact. To address this, noise conditional score matching adds Gaussian noise of arbitrary variance to the data and learns a noise-dependent score model. A single distribution is learned to approximate the data density in all noise regimes, which provides greater information to the model for learning low density regions.

To this end, the noise-added data model is

$$p(y|\sigma) = \int p(y|x, \sigma)p(x)dx \approx \frac{1}{N} \sum_{i=1}^N \mathcal{N}(y|x_i, \sigma^2 I).$$

Below, we will write a sample $y \sim p(y|\sigma)$ as $y = x + \xi$ where $x \sim \sum_{i=1}^N \frac{1}{N} \delta_{x_i}$ and $\xi \sim \mathcal{N}(0, \sigma^2 I)$. We modify our density to incorporate the parameter σ as follows,

$$q_\theta(y|\sigma) \propto \exp\{\theta^\top \phi_\sigma(y)\} \mathcal{N}(y|\mu, \Sigma_\sigma), \quad (17)$$

$$\phi_\sigma(y) = \sqrt{2/S} \cos(Zy/\gamma_\sigma + c) \quad (18)$$

$$\phi'_\sigma(y) = -\sqrt{2/S} \sin(Zy/\gamma_\sigma + c) \quad (19)$$

$$\gamma_\sigma := \sqrt{\gamma^2 + \sigma^2}, \quad \Sigma_\sigma = \Sigma + \sigma^2 I \quad (20)$$

We observe that the noise added to x is naturally incorporated in q_θ in two places: 1) By expanding the variance of the base Gaussian measure to expand the data region, and 2) by increasing the kernel width to learn the Gaussian process at multiple scales. Using the shared θ learned for all $\sigma > 0$, we can then evaluate q_θ at arbitrary resolution, e.g., $q_\theta(x) = q_\theta(y|\sigma = 0)$ since $\phi_0(y) = \phi(x)$.

With this modification, the standard noise conditional Fisher divergence objective is

$$\mathcal{L}_\sigma = \frac{1}{2} \sum_{i=1}^N \mathbb{E}_{p(\xi|\sigma)} [\|\nabla_x \ln q_\theta(x_i + \xi)\|^2] + \sum_{i=1}^N \mathbb{E}_{p(\xi|\sigma)} [\text{trace}(\nabla_{xx}^2 \ln q_\theta(x_i + \xi))], \quad (21)$$

where the derivatives in our case are given in Equations 7 and 8. We next show that these expectations can be solved analytically and a closed form solution exists for solving $\theta_{\text{FD}\sigma} = \arg \min_\theta \mathbb{E}_{p(\sigma)} [\mathcal{L}_\sigma] + \frac{\lambda}{2} \theta^\top \theta$, for a discretized distribution $\sigma \sim p(\sigma)$ defined later.

1) *Derivation of expectations:* From Equations 7, 8 and 21, four unique expectations arise. For the expectation of $\cos(z^\top y/\gamma_\sigma + c)$, where $y = x + \xi$ and $\xi \sim \mathcal{N}(0, \sigma^2 I)$,¹ we represent the argument as follows,

$$z^\top y/\gamma_\sigma + c \stackrel{d}{=} \epsilon + \chi_\sigma, \\ \chi_\sigma := z^\top x/\gamma_\sigma + c, \quad \epsilon \sim \mathcal{N}(0, \frac{\sigma^2}{\gamma^2 + \sigma^2} \|z\|^2).$$

Letting $j = \sqrt{-1}$, the MGF of a univariate Gaussian can be used to derive the following expectation,

$$\begin{aligned} \mathbb{E}[\cos(\epsilon + \chi_\sigma)] &= \text{Re} (e^{j\chi_\sigma} \mathbb{E}_{p(\epsilon|\sigma)} [e^{j\epsilon}]) \\ &= \exp\left(-\frac{\|z\|^2}{2} \frac{\sigma^2}{\gamma^2 + \sigma^2}\right) \cos(\chi_\sigma). \end{aligned} \quad (22)$$

Similarly, $\mathbb{E}[\sin(\epsilon + \chi_\sigma)]$ is solved using the imaginary component by replacing \cos in Equation 22 with \sin .

¹To reduce notation, we write y instead of y_σ . The accompanying γ_σ will indicate the value of σ used to generate y .

TABLE I: List of Expectations (also see Eqs. 18,19,24–26)

$\mathbb{E}[\phi_\sigma(y)]$	$= \delta_\sigma \odot \phi_\sigma(x)$
$\mathbb{E}[\phi'_\sigma(y)]$	$= \delta_\sigma \odot \phi'_\sigma(x)$
$\mathbb{E}[\phi'_\sigma(y)\phi'_\sigma(y)^\top]$	$= \frac{1}{2}(\Delta_\sigma^- - \Delta_\sigma^+) \odot \phi_\sigma(x)\phi_\sigma(x)^\top$ $+ \frac{1}{2}(\Delta_\sigma^- + \Delta_\sigma^+) \odot \phi'_\sigma(x)\phi'_\sigma(x)^\top$
$\mathbb{E}[(Z\Sigma_\sigma^{-1}\xi) \odot \phi'_\sigma(y)]$	$= -\frac{\sigma^2}{\gamma_\sigma} \delta_\sigma \odot \ Z\Sigma_\sigma^{-\frac{1}{2}}\ ^2 \odot \phi_\sigma(x)$

A third expectation arises of the form $\mathbb{E}[\phi'_{\sigma s}\phi'_{\sigma s'}]$. We use the identity $\sin(\alpha)\sin(\beta) = \frac{1}{2}(\cos(\alpha - \beta) - \cos(\alpha + \beta))$, where $\alpha = z_s^\top \xi/\gamma_\sigma + \chi_{\sigma s}$ and $\beta = z_{s'}^\top \xi/\gamma_\sigma + \chi_{\sigma s'}$, and again $\chi_{\sigma s} := z_s^\top x/\gamma_\sigma + c_s$. The expectation of these cosines follows a similar derivation as above and results in,

$$\begin{aligned} \mathbb{E}[\phi'_{\sigma s}(y)\phi'_{\sigma s'}(y)] &= \\ &\frac{1}{S} \exp\left(-\frac{\sigma^2\|z_s - z_{s'}\|^2}{2(\gamma^2 + \sigma^2)}\right) \cos(\chi_{\sigma s} - \chi_{\sigma s'}) \\ &- \frac{1}{S} \exp\left(-\frac{\sigma^2\|z_s + z_{s'}\|^2}{2(\gamma^2 + \sigma^2)}\right) \cos(\chi_{\sigma s} + \chi_{\sigma s'}) \end{aligned}$$

for all $s, s' \in \{1, \dots, S\}$, including $s = s'$. Using the identity $\cos(\alpha \pm \beta) = \cos \alpha \cos \beta \mp \sin \alpha \sin \beta$, this can be simplified for faster computation as shown later.

A final expectation is of the cross term in the square of the noise-added Equation 7. This expectation takes the form $\mathbb{E}_{p(\xi|\sigma)}[\xi^\top \Sigma_\sigma^{-1} z \sin(\xi^\top z/\gamma_\sigma + \chi_\sigma)]$. We solve this by writing vector products in sum form over the dimensions of ξ and solving D separate expectations. Using the shorthand $g(\xi) = \xi^\top z/\gamma_\sigma + \chi_\sigma$, and recalling that χ_σ is also a function of z , we solve by using the equality

$$\mathbb{E}[\xi_d \sin g(\xi)] = -x_d \mathbb{E} \sin g(\xi) - \gamma_\sigma (\partial/\partial z_d) \mathbb{E} \cos g(\xi).$$

After cancellations, and using the previous expectations for \sin and \cos , the total expectation is

$$\begin{aligned} \sum_{d=1}^D (\Sigma_\sigma^{-1} z)_d \mathbb{E}[\xi_d \sin(\xi^\top z/\gamma_\sigma + \chi_\sigma)] &= \\ \frac{\sigma^2}{\gamma_\sigma} (z^\top \Sigma_\sigma^{-1} z) \exp\left(-\frac{\|z\|^2}{2} \frac{\sigma^2}{\gamma^2 + \sigma^2}\right) \cos\left(\frac{z^\top x}{\gamma_\sigma} + c\right). \end{aligned} \quad (23)$$

We summarize all relevant expectations in vector form in Table I, where we use the following definitions:

$$\delta_\sigma(s) = \exp(-\frac{1}{2}(\sigma/\gamma_\sigma)^2 \|z_s\|^2), \quad (24)$$

$$\Delta_\sigma^+(s, s') = \exp(-\frac{1}{2}(\sigma/\gamma_\sigma)^2 \|z_s + z_{s'}\|^2), \quad (25)$$

$$\Delta_\sigma^-(s, s') = \exp(-\frac{1}{2}(\sigma/\gamma_\sigma)^2 \|z_s - z_{s'}\|^2), \quad (26)$$

where δ_σ is a vector and Δ_σ^+ and Δ_σ^- are matrices. Again, our definitions described previously are $\gamma_\sigma = \sqrt{\gamma^2 + \sigma^2}$, $\|ZM\|^2 \equiv (\|Mz_1\|^2, \dots, \|Mz_S\|^2)^\top$ and $\Sigma_\sigma = \Sigma + \sigma^2 I$. As previously defined in Equation 18, the RFF vector ϕ_σ indicates that the kernel width γ_σ is used, while (z, c) are shared for all values of σ .

2) *Algorithm summary and discussion:* We can now calculate the noise conditional objective function to be optimized. We use a uniform continuous distribution on $\sigma \in [\frac{\gamma}{D}, \sigma_{\max} + \frac{\gamma}{D}]$ approximated at H evenly spaced points starting at γ and terminating at $\frac{H-1}{H} \sigma_{\max} + \frac{\gamma}{D}$. The value of σ_{\max} is a parameter to be set. The minimum value $\frac{\gamma}{D} \ll \sigma_{\max}$ is the kernel width, which we empirically found resolves GP fluctuation issues that

Algorithm 3 Noise conditional Fisher TGP estimation

Require: Data $\{x_1, \dots, x_N\}, x \in \mathbb{R}^D$.

Model parameters $\gamma > 0, \lambda > 0, \mu \in \mathbb{R}^D, \Sigma \in \mathbb{S}_{++}^d$.

Approximation parameters $\sigma_{\max} > 0, \{H, S\} \in \mathbb{Z}_+$

- 1: Sample $z_s \sim \mathcal{N}(0, I_d), c_s \sim \text{Unif}(0, 2\pi), s = 1 : S$
- 2: Define $Z = [z_1, \dots, z_S]^\top$ and $c = (c_1, \dots, c_S)^\top$
- 3: Def. $\|ZM\|^2 = (\|Mz_1\|^2, \dots, \|Mz_S\|^2)^\top, M \in \mathbb{S}_{++}^d$
- 4: Define $\gamma_\sigma = \sqrt{\gamma^2 + \sigma^2}$ and $\Sigma_\sigma = \Sigma + \sigma^2 I$ for values of σ in the set $\Omega_\sigma = \{\frac{\gamma}{D} + \frac{h-1}{H}\sigma_{\max} : h = 1, \dots, H\}$
- 5: For data $\{x_i\}_{i=1:N}$ and each $\sigma \in \Omega_\sigma$, calculate RFF vectors $\phi_\sigma(x_i)$ and $\phi'_\sigma(x_i)$ as in Eqs 18 & 19, and

$$\begin{aligned}\Phi'_\sigma &= \sum_i \phi'_\sigma(x_i) \phi'_\sigma(x_i)^\top \\ \Phi_\sigma &= \sum_i \phi_\sigma(x_i) \phi_\sigma(x_i)^\top \\ \psi'_\sigma &= \sum_i \phi'_\sigma(x_i) \odot Z \Sigma_\sigma^{-1} (x_i - \mu) \\ \psi_\sigma &= \sum_i \phi_\sigma(x_i)\end{aligned}$$

- 6: Using definitions of $\delta_\sigma, \Delta_\sigma^-$ and Δ_σ^+ in Eqs 24—26, calculate the matrix A and vector b as follows

$$\begin{aligned}A &= \sum_{\sigma \in \Omega_\sigma} \frac{1}{2\gamma_\sigma^2} (\Delta_\sigma^- + \Delta_\sigma^+) \odot \Phi'_\sigma \\ &+ \sum_{\sigma \in \Omega_\sigma} \frac{1}{2\gamma_\sigma^2} (\Delta_\sigma^- - \Delta_\sigma^+) \odot \Phi_\sigma \\ b &= \sum_{\sigma \in \Omega_\sigma} \frac{1}{\gamma_\sigma} \delta_\sigma \odot \psi'_\sigma \\ &+ \sum_{\sigma \in \Omega_\sigma} \frac{1}{\gamma_\sigma^2} \|Z(I - \sigma^2 \Sigma_\sigma^{-1})^{\frac{1}{2}}\|^2 \odot \delta_\sigma \odot \psi_\sigma\end{aligned}$$

- 7: Solve directly or, e.g., with conjugate gradients,

$$\theta_{\text{FD}\sigma} = (\lambda H I + Z Z^\top \odot A)^{-1} b$$

return $\theta_{\text{FD}\sigma}, Z, c, \gamma, \mu, \Sigma$

occasionally occur in large regions of no data when $\sigma \rightarrow 0$. Without the prior,

$$\mathcal{L} = \mathbb{E}_{p(\sigma)}[\mathcal{L}_\sigma] \approx \frac{1}{H} \sum_{h=1}^H \mathcal{L}_{\frac{\gamma}{D} + \frac{h-1}{H}\sigma_{\max}}. \quad (27)$$

The gradient \mathcal{L}_σ for each discretized value of σ is

$$\begin{aligned}\nabla_\theta \mathcal{L}_\sigma &= -\frac{1}{\gamma_\sigma^2} \|Z\|^2 \odot \sum_{i=1}^N \mathbb{E}[\phi_\sigma(x_i + \xi_i)] \quad (28) \\ &- \frac{1}{\gamma_\sigma} \sum_{i=1}^N \mathbb{E}[\phi'_\sigma(x_i + \xi_i)] \odot Z \Sigma_\sigma^{-1} (x_i - \mu) \\ &- \frac{1}{\gamma_\sigma} \sum_{i=1}^N \mathbb{E}[(Z \Sigma_\sigma^{-1} \xi_i) \odot \phi'_\sigma(x_i + \xi_i)] \\ &+ \left(\frac{1}{\gamma_\sigma^2} Z Z^\top \odot \sum_{i=1}^N \mathbb{E}[\phi'_\sigma(x_i + \xi_i) \phi'_\sigma(x_i + \xi_i)^\top] \right) \theta.\end{aligned}$$

These terms parallel Equation 10 for the noise-free case. Using the expectations in Table I and including the Gaussian prior regularization of θ with parameter λ , the closed-form solution for θ that minimizes $\frac{1}{H} \sum_{h=1}^H \mathcal{L}_{\frac{\gamma}{D} + \frac{h-1}{H}\sigma_{\max}} + \frac{\lambda}{2} \theta^\top \theta$ is given in Algorithm 3. We observe that Algorithm 2 results as a special case when $\sigma \in \{0\}$.

C. Variational Predictive Distribution

As an alternative approach, we propose modeling uncertainty in θ and constructing the predictive distribution $p(x|x_1, \dots, x_N)$, with the same goal of eliminating artificially large densities in $p_\theta(x)$ that result from a point estimate of

θ . Since the log-linear form of our score uniquely allows for the predictive distribution to be approximated in closed form, it provides an alternative to the noise conditional framework used to learn deeper score functions.

To this end, we observe that the quadratic form in θ of the Fisher divergence in Equation 6, combined with the Gaussian prior on θ suggests a Gaussian posterior for θ . Since the Fisher divergence is not a proper log likelihood, we instead approximate the posterior by maximizing a variational ELBO-type function,

$$\mathcal{L}(q(\theta)) = \mathbb{E}_{q(\theta)} \left[-\frac{1}{2\eta} \mathbb{E}_{p(x)} \left\| \nabla_x \ln \frac{p(x)}{q_\theta(x)} \right\|^2 + \ln \frac{p(\theta)}{q(\theta)} \right].$$

Here, the log likelihood of the typical ELBO is replaced with the negative Fisher divergence. We also include an additional variational tempering (VT) parameter η , originally proposed by Mandt et al. [32] to anneal the ELBO for better local optimal learning of $q(\theta)$. In VT, η decreases to 1 as a function of iteration to ensure optimization of the desired ELBO; since we will be able to solve for the optimal $q(\theta)$ in closed form, we instead use η to perform a necessary regularization to balance the Fisher and KL divergence terms, which we discuss later.

Following the generic derivations of variational inference theory [33], the optimal $q(\theta)$ is

$$q(\theta) \propto \exp \left[-\frac{1}{2\eta} \mathbb{E}_{p(x)} \left\| \nabla_x \ln \frac{p(x)}{q_\theta(x)} \right\|^2 \right] p(\theta). \quad (29)$$

Because the Fisher divergence consists of terms linear and quadratic in θ , as shown in Section III-A, the solution to $q(\theta)$ is the following multivariate Gaussian,

$$\begin{aligned}q(\theta) &= \mathcal{N}(\theta | \hat{\mu}, \hat{\Sigma}) \quad (30) \\ \hat{\Sigma} &= \left(\lambda I + \frac{1}{\eta \gamma^2} Z Z^\top \odot \Phi' \right)^{-1} \\ \hat{\mu} &= (\lambda \gamma^2 \eta I + Z Z^\top \odot \Phi')^{-1} (\gamma \psi' + \|Z\|^2 \odot \psi).\end{aligned}$$

We use the definitions of Φ', ψ and ψ' in Algorithm 2. We also observe a similar parallel between ridge regression and Bayesian linear regression from the perspective of θ in the relationship between $\hat{\mu}$ and the solution to Algorithm 2, which has a MAP interpretation in this context.

Let $X = \{x_1, \dots, x_N\}$. The predictive distribution is

$$q(x|X) \approx \int q_\theta(x) q(\theta) d\theta$$

and we recall that $q_\theta(x) = \frac{\exp\{\theta^\top \phi(x)\} \mathcal{N}(x|\mu, \Sigma)}{\int \exp\{\theta^\top \phi(x)\} \mathcal{N}(x|\mu, \Sigma) dx}$.

The integral of this variational predictive distribution is intractable because θ appears in the intractable denominator of $q_\theta(x)$. To this end, we introduce the following MGF approximation of the normalizing constant of $q_\theta(x)$,

$$\begin{aligned}\mathbb{E}_{x \sim \mathcal{N}(x|\mu, \Sigma)} [\exp\{\theta^\top \phi(x)\}] &\approx \exp\{\theta^\top \mu_\phi + \frac{1}{2} \theta^\top \Sigma_\phi \theta\}, \\ \mu_\phi &= \mathbb{E}[\phi(x)], \quad \Sigma_\phi = \mathbb{E}[\phi(x) \phi(x)^\top] - \mu_\phi \mu_\phi^\top. \quad (31)\end{aligned}$$

Algorithm 4 Fisher variational predictive TGP distribution

Require: Data $x \in \mathbb{R}^D$, kernel width $\gamma > 0$, param $\lambda > 0$, $S \in \mathbb{Z}_+$, base params $\mu \in \mathbb{R}^D$, $\Sigma \in \mathbb{S}_{++}^D$, variational tempering param $\eta > 0$ (we set $\eta = 1/\gamma^2$)

- 1: Sample $z_s \sim \mathcal{N}(0, I_d)$, $c_s \sim \text{Unif}(0, 2\pi)$, $s = 1 : S$
- 2: Def $Z = [z_1, \dots, z_S]^\top$, $\|Z\|^2 = (\|z_1\|^2, \dots, \|z_S\|^2)^\top$
- 3: Construct each $\phi'(x_i)$ and $\phi(x_i) = -\phi''(x_i)$ (Eq. 9)
- 4: Using all data, calculate Φ' , ψ' , ψ as in Algorithm 2.
- 5: Calculate $\hat{\mu}$, $\hat{\Sigma}$, μ_ϕ , Σ_ϕ (Eqs. 30, 32 & 33)
- 6: Construct the approximate predictive distribution

$$p(x|X) \propto \mathcal{N}(x|\mu, \Sigma) e^{\frac{1}{2}\phi(x)^\top \mathbf{M}^{-1}\phi(x) - \phi(x)^\top \mathbf{M}^{-1}\mathbf{m}}$$

$$\mathbf{m} = \mu_\phi - \hat{\Sigma}^{-1}\hat{\mu}, \quad \mathbf{M} = \Sigma_\phi + \hat{\Sigma}^{-1}$$

return unscaled $p(x|X)$ with params μ , Σ , \mathbf{m} , \mathbf{M} , Z , c

Using similar derivations as discussed in Section III-B for the noise conditional model, we can show that

$$\mu_\phi(s) = \exp\left\{-\frac{1}{2\gamma^2} z_s^\top \Sigma z_s\right\} \phi_s(\mu) \quad (32)$$

$$\begin{aligned} \Sigma_\phi &= \frac{1}{2}(\Delta^- + \Delta^+) \odot \phi(\mu)\phi(\mu)^\top \\ &\quad + \frac{1}{2}(\Delta^- - \Delta^+) \odot \phi'(\mu)\phi'(\mu)^\top - \mu_\phi \mu_\phi^\top \\ \Delta_{ss'}^+ &\equiv \exp\left\{-\frac{1}{2\gamma^2}(z_s + z_{s'})^\top \Sigma(z_s + z_{s'})\right\} \\ \Delta_{ss'}^- &\equiv \exp\left\{-\frac{1}{2\gamma^2}(z_s - z_{s'})^\top \Sigma(z_s - z_{s'})\right\}. \end{aligned} \quad (33)$$

With this approximation, the predictive distribution becomes

$$q(x|X) \propto \mathcal{N}(x|\mu, \Sigma) \int e^{\theta^\top (\phi(x) - \mu_\phi) - \frac{1}{2}\theta^\top \Sigma_\phi \theta} \mathcal{N}(\theta|\hat{\mu}, \hat{\Sigma}) d\theta,$$

which can be solved up to a proportionality constant. After integrating, the approximate predictive distribution is proportional to

$$\begin{aligned} q(x|X) &\propto \mathcal{N}(x|\mu, \Sigma) e^{\frac{1}{2}\phi(x)^\top \mathbf{M}^{-1}\phi(x) - \phi(x)^\top \mathbf{M}^{-1}\mathbf{m}}, \\ \mathbf{m} &= \mu_\phi - \hat{\Sigma}^{-1}\hat{\mu}, \quad \mathbf{M} = \Sigma_\phi + \hat{\Sigma}^{-1}. \end{aligned} \quad (34)$$

We summarize our *Fisher variational predictive distribution* (FVPD) in Algorithm 4.

1) *Discussion:* We can observe some properties of Equation 34 to connect it with Algorithm 2 and help guide setting of η . First we note that, since γ^2 can be very small, $\mathbf{M}^{-1}\mathbf{m} \approx -\hat{\mu}$ and $\phi(x)^\top \mathbf{M}^{-1}\phi(x) \approx 0$ when $\eta = 1$. Effectively, the predictions of Algorithm 2 and Algorithm 4 are the same since $\hat{\mu} = \theta_{\text{FD}}$. In this scenario, we empirically observed nearly identical results as Algorithm 2 in terms of low-density inaccuracy, since a huge $1/\gamma^2$ scaling removes uncertainty in θ . To eliminate this effect, the tempering parameter η can act as a regularizer to balance the Fisher and KL divergence terms of the ELBO. We found that setting $\eta = 1/\gamma^2$ can remove the undesirable impacts of γ in Equation 30.

We also observe that the predictive distribution in Equation 34 can only be solved up to a normalizing constant, since the integral over x remains intractable, which requires additional considerations similar to other unnormalized score models. One discretization option here is to sample $x_i \sim_{iid} \mathcal{N}(x|\mu, \Sigma)$ many

times and approximate $p(x_i|X) \propto \exp\{\frac{1}{2}\phi(x_i)^\top \mathbf{M}^{-1}\phi(x_i) - \phi(x_i)^\top \mathbf{M}^{-1}\mathbf{m}\}$ on these samples. For generative models where one dimension of x is predicted conditioned on values for the others, a 1D grid approximation of Equation (34) can be made over the free dimension.

IV. EXPERIMENTS

We evaluate the four algorithms in this paper on nine low dimensional benchmark data sets and three other data sets. These include LCD, CA House, Bikeshare, FICO, HIGGS, MIMIC2, Credit, Adult and Churn from the UCI repository, along with a projected MNIST data set and two simulated 2D data sets. The dimensionality and training size of the benchmark data are indicated in Table II, with several thousand additional data held out for testing. For all experiments, we set $S = 1000$, $\gamma = \frac{1}{10}\sqrt{\text{tr}(\nabla(x))}$, and $\lambda = 10$, except for the vanilla Fisher divergence, where $\lambda = 100$. We set μ and Σ in the base normal distribution to be their empirical values from the data. For Fisher divergence we optimized these values after learning θ_{FD} without reiterating. For the noise conditional model we set $\sigma_{\text{max}} = \sqrt{\text{tr}(\nabla(x))/D}$.

The four inference algorithms for the GP-tiled density are MAP, Fisher Divergence (FD), Noise Conditional Fisher Divergence (NCFD), and Fisher Variational Predictive Distribution (FVPD). Considering its similarity with Kernel Density Estimation, we also show a qualitative result comparing with $p(x|X) \propto \sum_{i=1}^N k(x, x_i)$ (KDE- ∞) and its approximation $p(x|X) \propto \phi(x)^\top [\sum_{i=1}^N \phi(x_i)]$ (KDE-RFF), which is very fast but inaccurate when S is small.

We first show qualitative results on dimensions 7 and 8 from the CA House data set due to its unique real world pattern. In Figure 1 we show the original data with 10K samples generated from each learned density super imposed. (The RHS of Figure 2 better visualizes the raw data.) In general, we see that the GP-tilted model is able to learn complex densities with a single vector $\theta \in \mathbb{R}^S$. MAP and FD underperform NCFD and FVPD in opposite directions. Compared with the standard NCFD model, our proposed FVPD is able to learn sharper densities by modeling “noise” (uncertainty) in the posterior of θ rather than in the noise-added data itself. KDE-RFF essentially failed for smaller S due to artifacts, which are still visible when $S=100,000$. The exact KDE also does well, but is based directly on the raw data. In Figure 2 we show the noise conditional density contours for (NCFD) as a function of decreasing σ .

In Figure 3 we show contour plots for the four learning approaches of our GP-tilted density using three other data sets: MNIST-60K projected onto its first two principal components, and XO and Smile synthetic data. For NCFD, we show the final data-level density not integrated over σ . Noticeable in FD algorithm are a tendency to learn high density values outside of the data region. This issue due to the lack of data to learn meaningful gradients is addressed as intended by the other Fisher approaches, although we observe that NCFD has issues with XO. We also note that MAP also performs well on these problems.

Model	LCD (5D, 10K)	CA (8D, 14K)	Bikeshare (12D, 11K)	FICO (36D, 7K)	HIGGS (28D, 50K)	MIMIC2 (17D, 16K)	Credit (30D, 182K)	Adult (14D, 21K)	Churn (19D, 5K)
FVPD	-0.751 ± 0.003	-6.62 ± 0.02	-1.97 ± 0.00	-3.59 ± 0.17	-3.99 ± 0.02	-2.77 ± 0.01	-4.60 ± 0.03	-2.09 ± 0.01	-2.57 ± 0.01
NCFD	-0.752 ± 0.003	-6.75 ± 0.00	-1.96 ± 0.01	-4.17 ± 0.05	-4.00 ± 0.02	-2.77 ± 0.01	-4.61 ± 0.02	-2.10 ± 0.01	-2.56 ± 0.01
FD	-0.764 ± 0.003	-7.26 ± 0.03	-2.00 ± 0.01	-3.63 ± 0.19	-4.01 ± 0.02	-2.94 ± 0.01	-4.61 ± 0.03	-2.10 ± 0.01	-2.67 ± 0.01
MAP	-0.752 ± 0.003	-6.43 ± 0.01	-1.97 ± 0.01	-3.98 ± 0.06	-4.02 ± 0.02	-2.79 ± 0.01	-4.64 ± 0.03	-2.10 ± 0.01	-2.56 ± 0.01

TABLE II: Average test log likelihood for the inference approaches described in Algorithms 1-4 for some common benchmark data sets. Dimensionality and training data size are indicated below the data name. Noise conditional and variational methods improve Fisher divergence learning, with our proposed variational predictive marginal likelihood often better than the noise conditional option. MAP performs well using this metric due to its similar objective function.

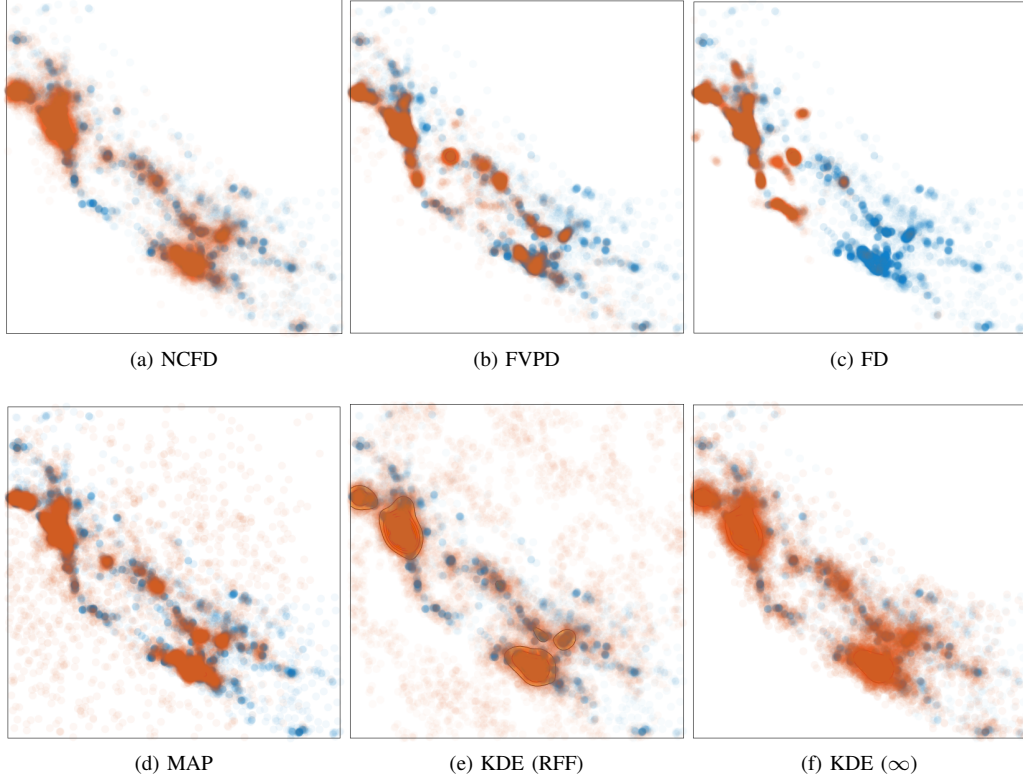


Fig. 1: Samples (orange) shown over data (blue) generated from (a) the noise conditional Fisher divergence (Algorithm 3), (b) the Fisher variational predictive distribution (Algorithm 4), (c) Fisher divergence (Algorithm 2), (d) MAP inference (Algorithm 1), (e,f) kernel density estimation (see text for discussion). We set $S = 1000$ for (a)-(d) and $S = 100K$ for (e), $\lambda = 10$ for (a,b,d) and $\lambda = 100$ for (c). All methods use the same kernel width γ .

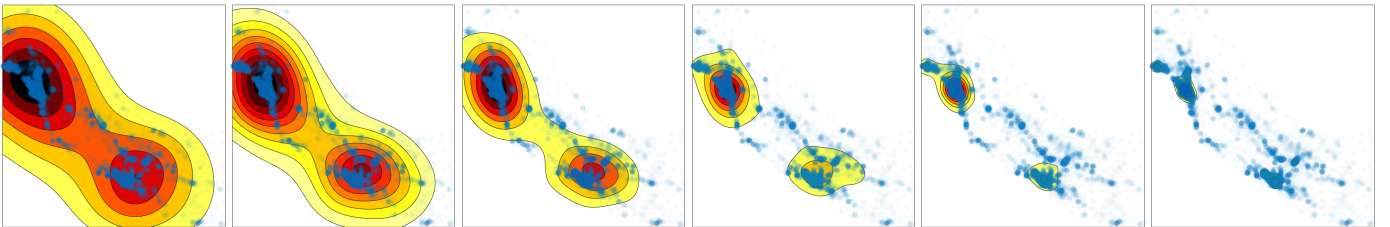


Fig. 2: Noise conditional density contours on CA House data for decreasing σ . For better visualization, Figure 1 shows samples from the final RHS density contour (NCFD), along with samples from the other learned methods.

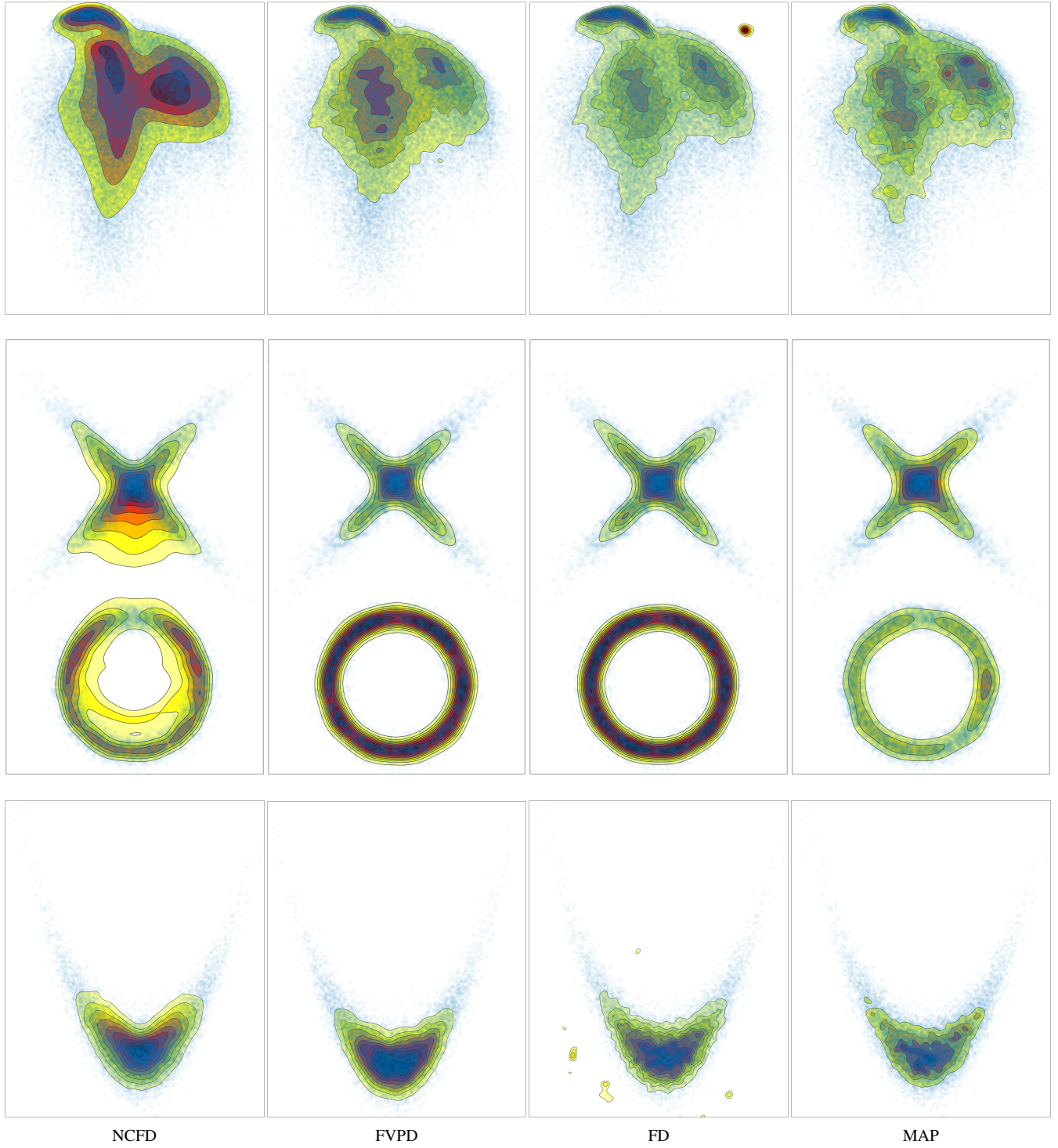


Fig. 3: Contour plots of GP-tilted density learned by each algorithm on three data sets. Data shown in light blue.

We also evaluate our algorithms quantitatively in Table II on 9 public benchmark data sets. We use the expected log (predictive) likelihood learned by the corresponding algorithm. Since all distributions can only be learned up to a proportionality constant, we approximate the log normalizer with $100K$

samples to allow for direct comparison. We note that KDE (not shown) performed worse generally, with KDE-RFF having significant issues with approximation artifacts. We observe that MAP generally performs very well, since it is based on the log likelihood and evaluated on test data very similar to

training data. Still, it is often beaten by Fisher divergence. We also observe that the basic Fisher divergence is often significantly worse than our uncertainty-informed versions. Of these, uncertainty captured by the model’s posterior distribution (FVPD) can frequently improve upon uncertainty captured by noise added to the data and modeled by the likelihood-based score function (NCFD).

V. CONCLUSION

We have proposed a GP-tilted density for low dimensional problems. Our Gaussian process makes use of the random Fourier feature representation for tractable nonparametric learning. We propose three Fisher divergence based learning algorithms, for which the GP-RFF score function is mathematically equivalent to a single layer neural network with known hidden layer parameters. Two features and contributions of our methods include:

- 1) With the exception of normalizing constants, all integrals and expectations are closed form, or easily approximated in closed form (Equation 31). The algorithms are therefore not iterative, but use sufficient statistics of the data.
- 2) We propose a variational approximation to the model posterior using an ELBO-like function based on the Fisher divergence and variational tempering. The corresponding predictive distribution on the data integrates out uncertainty in the model parameter rather than by adding noise to the data, giving an alternative to noise-conditional Fisher divergence methods for our model.

In future work, we plan to adapt our GP-tilted score model and associated algorithms to real world applications and investigate methods for learning the important regularization parameters λ (GP prior) and η (variational tempering) and kernel width γ . While we provided suggestions for setting η as a function of γ , these parameter settings were still empirically hand tuned and can be further optimized.

REFERENCES

- [1] H. Larochelle and I. Murray, “The neural autoregressive distribution estimator,” in *Artificial Intelligence and Statistics*, 2011.
- [2] M. Germain, K. Gregor, I. Murray, and H. Larochelle, “Made: Masked autoencoder for distribution estimation,” in *International Conference on Machine Learning*, 2015.
- [3] A. van den Oord, N. Kalchbrenner, L. Espeholt, O. Vinyals, A. Graves *et al.*, “Conditional image generation with PixelCNN decoders,” in *Advances in Neural Information Processing Systems*, 2016.
- [4] A. van den Oord, S. Dieleman, H. Zen, K. Simonyan, O. Vinyals, A. Graves, N. Kalchbrenner, A. W. Senior, and K. Kavukcuoglu, “Wavenet: A generative model for raw audio,” in *Speech Synthesis Workshop*, 2016.
- [5] D. P. Kingma, “Auto-encoding variational Bayes,” *arXiv preprint arXiv:1312.6114*, 2013.
- [6] D. J. Rezende, S. Mohamed, and D. Wierstra, “Stochastic backpropagation and approximate inference in deep generative models,” in *International Conference on Machine Learning*, 2014.
- [7] Y. Song and D. P. Kingma, “How to train your energy-based models,” *arXiv preprint arXiv:2101.03288*, 2021.
- [8] D. Rezende and S. Mohamed, “Variational inference with normalizing flows,” in *International Conference on Machine Learning*, 2015.
- [9] L. Dinh, J. Sohl-Dickstein, and S. Bengio, “Density estimation using Real NVP,” in *International Conference on Learning Representations*, 2017.
- [10] D. P. Kingma, T. Salimans, R. Jozefowicz, X. Chen, I. Sutskever, and M. Welling, “Improved variational inference with inverse autoregressive flow,” in *Advances in Neural Information Processing Systems*, 2016.
- [11] D. P. Kingma and P. Dhariwal, “Glow: Generative flow with invertible 1x1 convolutions,” in *Advances in Neural Information Processing Systems*, 2018.
- [12] I. Goodfellow, J. Pouget-Abadie, M. Mirza, B. Xu, D. Warde-Farley, S. Ozair, A. Courville, and Y. Bengio, “Generative adversarial nets,” in *Advances in Neural Information Processing Systems*, 2014.
- [13] Y. Song and S. Ermon, “Generative modeling by estimating gradients of the data distribution,” in *Advances in Neural Information Processing Systems*, 2019.
- [14] Q. Liu, J. Lee, and M. Jordan, “A kernelized stein discrepancy for goodness-of-fit tests,” in *International Conference on Machine Learning*, 2016.
- [15] A. Hyvärinen and P. Dayan, “Estimation of non-normalized statistical models by score matching,” *Journal of Machine Learning Research*, vol. 6, no. 4, 2005.
- [16] P. Vincent, “A connection between score matching and denoising autoencoders,” *Neural Computation*, vol. 23, no. 7, pp. 1661–1674, 2011.
- [17] Y. Song, S. Garg, J. Shi, and S. Ermon, “Sliced score matching: A scalable approach to density and score estimation,” in *Uncertainty in Artificial Intelligence*, 2020.
- [18] F. Cole and Y. Lu, “Score-based generative models break the curse of dimensionality in learning a family of sub-gaussian probability distributions,” in *International Conference on Learning Representations*, 2024.
- [19] Y. Song, L. Shen, L. Xing, and S. Ermon, “Solving inverse problems in medical imaging with score-based generative models,” in *International Conference on Learning Representations*, 2022.
- [20] A. Jalal, M. Arvinte, G. Daras, E. Price, A. G. Dimakis, and J. Tamir, “Robust compressed sensing MRI with deep generative priors,” in *Advances in Neural Information Processing Systems*, 2021.
- [21] J. Hensman, M. Zwiefel, and N. D. Lawrence, “Tilted variational Bayes,” in *Artificial Intelligence and Statistics*, 2014.
- [22] V. Dutordoir, H. Salimbeni, J. Hensman, and M. Deisenroth, “Gaussian process conditional density estimation,” in *Advances in Neural Information Processing Systems*, 2018.
- [23] G. Floto, S. Kremer, and M. Nica, “The tilted variational

- autoencoder: Improving out-of-distribution detection,” in *International Conference on Learning Representations*, 2023.
- [24] L. Wenliang, D. J. Sutherland, H. Strathmann, and A. Gretton, “Learning deep kernels for exponential family densities,” in *International Conference on Machine Learning*, 2019.
 - [25] Z. Wang, S. Cheng, L. Yueru, J. Zhu, and B. Zhang, “A Wasserstein minimum velocity approach to learning unnormalized models,” in *Artificial Intelligence and Statistics*, 2020.
 - [26] L. Pacchiardi and R. Dutta, “Score matched neural exponential families for likelihood-free inference,” *Journal of Machine Learning Research*, vol. 23, no. 38, pp. 1–71, 2022.
 - [27] O. Tsymboi, Y. Kapushev, E. Burnaev, and I. Oseledets, “Denoising score matching via random fourier features,” *IEEE Access*, vol. 10, pp. 34 154–34 169, 2022.
 - [28] A. Rahimi and B. Recht, “Random features for large-scale kernel machines,” in *Advances in Neural Information Processing Systems*, 2008.
 - [29] W. Zhang, B. Barr, and J. Paisley, “Gaussian process neural additive models,” in *AAAI Conference on Artificial Intelligence*, 2024.
 - [30] —, “Gaussian process neural network embeddings for collaborative filtering,” in *IEEE International Conference on Machine Learning and Applications*, 2024.
 - [31] C. K. Williams and C. E. Rasmussen, *Gaussian Processes for Machine Learning*. MIT Press, 2006, vol. 2, no. 3.
 - [32] S. Mandt, J. McInerney, F. Abrol, R. Ranganath, and D. Blei, “Variational tempering,” in *Artificial Intelligence and Statistics*, 2016.
 - [33] C. M. Bishop, *Pattern Recognition and Machine Learning*. Springer, 2006.